Appendix B

Models for Calculating Lung Burdens

B.1. INTRODUCTION

1

2

3

4

5

6

7

8

9

10

11

12

13

14

15

16

17

18

19

20

21

22

23

24

25

26

27

28

29

30 31

32

33

34

35

36

As discussed in Chapter 4, the lung burden of diesel exhaust particles (DEPs) during exposure is determined by both the amount and site of particle deposition in the lung and, subsequently, by rates of translocation and clearance from the deposition sites. Mathematical models have often been used to complement experimental studies in estimating the lung burdens of inhaled particles in different species under different exposure conditions. This section presents a mathematical model that simulates the deposition and clearance of DEPs in the lungs of rats and humans.

Diesel particles are aggregates formed from primary spheres 15-30 nm in diameter. The aggregates are irregularly shaped and range in size from a few molecular diameters to tens of microns. The mass median aerodynamic diameter (MMAD) of the aggregates is approximately 0.2 µm. The primary sphere consists of a carbonaceous core (soot) on which numerous kinds of organic compounds are adsorbed. The organics normally account for 10% to 30% of the particle mass. However, the exact size distribution of DEPs and the specific composition of the adsorbed organics depend upon many factors, including engine design, fuels used, engine operating conditions, and the thermodynamic process of exhaust. The physical and chemical characteristics of DEPs have been reviewed extensively by Amann and Siegla (1982) and Schuetzle (1983).

Four mechanisms deposit diesel particles within the respiratory tract during exposure: impaction, sedimentation, interception, and diffusion. The contribution from each mechanism to deposition, however, depends upon lung structure and size, the breathing condition of the subject, and particle size distribution. Under normal breathing conditions, diffusion is the most dominant mechanism. The other three mechanisms play only a minor role.

Once DEPs are deposited in the respiratory tract, both the carbonaceous cores and the adsorbed organics of the particles will be removed from the deposition sites as described in Chapter 4. There are two mechanisms that facilitate this removal: (a) mechanical clearance, provided by mucociliary transport in the ciliated conducting airways as well as macrophage phagocytosis and migration in the nonciliated airways; and (b) clearance by dissolution. As the carbonaceous soot of DEPs is insoluble, it is removed from the lung primarily by mechanical clearance, whereas the adsorbed organics are removed principally by dissolution.

B.2. PARTICLE MODEL

To develop a mathematical model that simulates the deposition and clearance of DEPs in the lung, an appropriate model for diesel particles must be introduced. For the deposition study, we employed an equivalent sphere model developed by Yu and Xu (1987) to simulate the dynamics and deposition of DEPs in the respiratory tract by various mechanisms. For the clearance study, we assume that a diesel particle is composed of three different material

components according to their characteristic clearance rates: (1) a carbonaceous core of approximately 80% of the particle mass; (2) absorbed organics of about 10% of particle mass, which are slowly cleared from the lung; and (3) adsorbed organics quickly cleared from the lung, accounting for the remaining 10% of particle mass. The presence of two discrete organic phases in the particle model is suggested by observations that the removal of particle-associated organics from the lung exhibits a biphasic clearance curve (Sun et al., 1984; Bond et al., 1986), as discussed in Chapter 4. This curve represents two major kinetic clearance phenomena: a fastphase organic washout with a half-time of a few hours, and a slow phase with a half-time that is a few hundred times longer. The detailed components involved in each phase are not known. It is possible that the fast phase consists of organics that are leached out primarily by diffusion mechanisms while the slow phase might include any or all of the following components: (a) organics that are "loosened" before they are released, (b) organics that have become intercalated in the carbon core and whose release is thus impeded, (c) organics that are associated for longer periods of time because of hydrophobic interaction with other organic-phase materials, (d) organics that have been ingested by macrophages and as a result effectively remain in the lung for a longer period of time because of metabolism by the macrophage (metabolites formed may interact with other cellular components), and (e) organics that have directly acted on cellular components, such as the formation of covalent bonds with DNA and other biological macromolecules to form adducts.

The above distinction of the organic components is largely mechanistic and does not specifically imply the actual nature of the organics adsorbed on the carbonaceous core; the distinction is made to account for the biphasic clearance of DEPs. However, this distinction is necessary in appreciating the dual-phase nature of DEPs. For aerosols made of pure organics, such as benzo(a)pyrene (BaP) and nitropyrene (NP) in the same size range of DEPs, Sun et al. (1984) and Bond et al. (1986) observed a nearly monophasic clearance curve. This might be explained by the absence of intercalative phenomena (a) and of hydrophobic interaction imposed by a heterogeneous mixture of organics (b). The measurement of a pure organic might also neglect that quantity which has become intracellular (c) or covalently bound (d).

B.3. COMPARTMENTAL LUNG MODEL

To study the transport and removal of DEPs from the lungs, we used a compartmental model consisting of four anatomical compartments: the nasopharyngeal or head (H), tracheobronchial (T), alveolar (A), and lung-associated lymph node (L), as shown in Figure B-1. In addition, we used two outside compartments B and G representing, respectively, the blood and gastrointestinal (GI) tract. The alveolar compartment in the model is obviously the most

1

2

3

4

5

6

7

8

9

10

11

12

13

14

15

16

17

18

19

20

21

22

23

24

25

26

27

28

29 30

31

32

33

34

Figure B-1. Compartmental model of DEP retention.

important for long-term retention studies. However, for short-term consideration, retentions in other lung compartments may also be significant. The presence of these lung compartments and the two outside compartments in the model therefore provides a complete description of all clearance processes involved.

In Figure B-1, $r_{H}^{(i)}$, $r_{T}^{(i)}$, and $r_{A}^{(i)}$ are, respectively, the mass deposition rates of DEP material component i (i=1 [core], 2 [slowly cleared organics], and 3 [rapidly cleared organics]) in the head, tracheobronchial, and alveolar compartments; and $\lambda_{XY}^{(i)}$ represents the transport rate of material

1

2

3

4

5

6

1 component i from any compartment X to any compartment Y. Let the mass fraction of material 2 component i of a diesel particle be fi. Then

$$r_H^{(i)} = f_i r_H \quad , ag{B-1}$$

3

$$r_T^{(i)} = f_i r_T$$
 (B-2)

4

$$r_A^{(i)} = f_i r_A \quad , \tag{B-3}$$

5 6

where r_H , r_T , and r_A are, respectively, the total mass deposition rates of DEPs in the H, T, and A compartments, determined from the equations:

8

7

$$r_H = c(TV)(RF)(DF)_H , \qquad (B-4)$$

9

$$r_T = c(TV)(RF)(DF)_T \quad , \tag{B-5}$$

10

$$r_A = c(TV)(RF)(DF)_A . (B-6)$$

11 12

13 14

15

16

In Equations B-4 to B-6, c is the mass concentration of DEPs in the air, TV is the tidal volume, RF is the respiratory frequency, and (DF)_H, (DF)_T, and (DF)_A are, respectively, the deposition fractions of DEPs in the H, T, and A compartments over a respiratory cycle. The values of (DF)_H, (DF)_T, and (DF)_A, which vary with the particle size, breathing conditions, and lung architecture, were determined from our deposition model (Yu and Xu, 1987).

17 18

The differential equations for $m_{XY}^{(i)}$, the mass of material component i in compartment X as a function of exposure time t, can be written as

19 20

Head (H)

21

$$\frac{dm_H^{(i)}}{dt} = r_H^{(i)} - \lambda_{HG}^{(i)} m_H^{(i)} - \lambda_{HB}^{(i)} m_H^{(i)} , \qquad (B-7)$$

22

Tracheobronchial (T)

$$\frac{dm_T^{(i)}}{dt} = r_T^{(i)} + \lambda_{AT}^{(i)} m_A^{(i)} - \lambda_{TG}^{(i)} m_T^{(i)} - \lambda_{TB}^{(i)} m_T^{(i)} , \qquad (B-8)$$

1 Alveolar (A)

$$\frac{dm_A^{(i)}}{dt} = r_A^{(i)} - \lambda_{AT}^{(i)} m_A^{(i)} - \lambda_{AL}^{(i)} m_A^{(i)} - \lambda_{AB}^{(i)} m_A^{(i)} , \qquad (B-9)$$

2 Lymph nodes (L)

$$\frac{dm_L^{(i)}}{dt} = \lambda_{AL}^{(i)} m_A^{(i)} - \lambda_{LB}^{(i)} m_L^{(i)} . \tag{B-10}$$

3 Equation B-9 may also be written as

$$\frac{dm_A^{(i)}}{dt} = r_A^{(i)} - \lambda_A^{(i)} m_A^{(i)} , \qquad (B-11)$$

4 where

$$\lambda_A^{(i)} = \lambda_{AT}^{(i)} + \lambda_{AL}^{(i)} + \lambda_{AB}^{(i)}$$
 (B-12)

- 5 is the total clearance rate of material component i from the alveolar compartment. In Equations
- 6 B-7 to B-10, we have assumed vanishing material concentration in the blood compartment to
- 7 calculate diffusion transport.
 - The total mass of the particle-associated organics in compartment X is the sum of $m_X^{(2)}$ and $m_X^{(3)}$ the total mass of DEPs in compartment X is equal to

$$m_{\rm Y} = m_{\rm Y}^{(1)} + m_{\rm Y}^{(2)} + m_{\rm Y}^{(3)}$$
 (B-13)

10 The lung burdens of diesel soot (core) and organics are defined, respectively, as

$$m_{Lung}^{(1)} = m_T^{(1)} + m_A^{(1)}$$
 (B-14)

11 and

14

15 16

17

8 9

$$m_{Lung}^{(2)+(3)} = m_T^{(2)} + m_A^{(2)} + m_T^{(3)} + m_A^{(3)}$$
 (B-15)

- 12 Because the clearance of diesel soot from compartment T is much faster than from compartment
- A, $m_T^{(1)} < m_A^{(1)}$ a short time after exposure, Equation B-14 leads to 13

$$m_{Lung}^{(1)} \cong m_A^{(1)}$$
 (B-16)

Solution to Equations B-7 to B-10 can be obtained once all the transport rates $\lambda_{XY}^{(i)}$ are known. When $\lambda_{XY}^{(i)}$ are constant, which is the case in linear kinetics, Equations B-7 to B-10 will have a solution that increases with time at the beginning of exposure but eventually saturates and reaches a steady-state value. This is the classical retention model developed by the International

Commission of Radiological Protection (ICRP, 1979). However, as discussed in Chapter 4, data have shown that when rats are exposed to DEPs at high concentration for a prolonged period, the diesel soot accumulates in various peribronchial and subpleural regions in the lung and the long-termed clearance is impaired. This is the so-called overload effect, observed also for other insoluble particles. The overload effect cannot be predicted by the classical ICRP model. Soderholm (1981) and Strom et al. (1987, 1988) have proposed a model to simulate this effect by adding a separate sequestrum compartment in the alveolar region. In the present approach, a single compartment for the alveolar region of the lung is used and the overload effect is accounted for by a set of variable transport rates $\lambda_{AD}^{(i)}$ $\lambda_{AD}^{(i)}$, and $\lambda_{AD}^{(i)}$ which are functions of m_A . The transport rates $\lambda_A^{(i)}$ and $\lambda_{AD}^{(i)}$ in Equations B-7 to B-10 can be determined directly from experimental data on lung and lymph node burdens, and $\lambda_{AD}^{(i)}$ and $\lambda_{AD}^{(i)}$ from Equation B-12.

B.4. SOLUTIONS TO KINETIC EQUATIONS

Equation B-11 is a nonlinear differential equation of $m_A^{(i)}$ with known function of $\lambda_A^{(i)}$. For diesel soot, this equation becomes

$$\frac{dm_A^{(1)}}{dt} = r_A^{(1)} - \lambda_A^{(1)}(m_A)m_A^{(1)} . \tag{B-17}$$

Because clearance of the particle-associated organics is much faster than diesel soot, $m_A^{(2)}$ and $m_A^{(3)}$ constitute only a very small fraction of the total particle mass (less than 1%) after a long exposure, and we may consider $\lambda_A^{(I)}$ as a function of $m_A^{(I)}$ alone. Equation B-17 is then reduced to a differential equation with $m_A^{(I)}$ the only dependent variable.

The general solution to Equation B-17 for constant $r_A^{(1)}$ at any time, t, can be obtained by the separation of variables to give

$$\int_0^{m_A^{(1)}} \frac{dm_A^{(1)}}{r_A^{(1)} - \lambda_A^{(1)} m_A^{(1)}} = t \quad . \tag{B-18}$$

If $r_A^{(I)}$ is an arbitrary function of t, Equation B-17 needs to be solved numerically such as by a Runge-Kutta method. Once $m_A^{(I)}$ is found, the other kinetic equations B-7 to B-10 for both diesel soot and the particle-associated organics can be solved readily, as they are linear equations. The solutions to these equations for constant $r_H^{(i)}$, $r_T^{(i)}$, and $r_A^{(i)}$ are given below:

26 Head (H)

$$m_H^{(i)} = r_H^{(i)}/\lambda_H^{(i)} + (m_{H0}^{(i)} - r_H^{(i)})/\lambda_H^{(i)}) \exp(-\lambda_H^{(i)} t)$$
 (B-19)

where
$$\lambda_H^{(i)} = \lambda_{HG}^{(i)} + \lambda_{HB}^{(i)}$$
 (B-20)

1 Tracheobronchial (T)

$$m_T^{(i)} = \exp(-\lambda_T^{(i)} t) \int_0^t (r_T^{(i)} + \lambda_{AT}^{(i)} m_A^{(i)}) \exp(\lambda_{AT}^{(i)} t) dt + m_{T0}^{(i)}$$
 (B-21)

where
$$\lambda_T^{(i)} = \lambda_{TG}^{(i)} + \lambda_{TB}^{(i)}$$
 (B-22)

Lymph nodes (L)

$$m_L^{(i)} = \exp(-\lambda_{LB}^{(i)} t) \int_0^t \lambda_{AL}^{(i)} m_A^{(i)} \exp(\lambda_{LB}^{(i)}) dt + m_{L0}^{(i)}$$
 (B-23)

In Equations B-19 to B-23, $m_{XO}^{(i)}$ represents the value of $m_X^{(i)}$ at t = 0.

In the sections to follow, the methods of determining $r_H^{(i)}$, $r_T^{(i)}$, and $r_A^{(i)}$, or $(DF)_H$, $(DF)_T$, and $(DF)_A$, $r_H^{(DF)}$, $r_T^{(DF)}$, and $r_A^{(DF)}$, as well as the values of $\lambda_{XY}^{(i)}$ in the compartmental lung model are presented.

B.5. DETERMINATION OF DEPOSITION FRACTIONS

The mathematical models for determining the deposition fractions of DEPs in various regions of the respiratory tract have been developed by Yu and Xu (1986, 1987) and are adopted in this report. Yu and Xu consider DEPs as a polydisperse aerosol with a specified mass median aerodynamic diameter (MMAD) and geometrical standard deviation σ_g . Each diesel particle is represented by a cluster-shaped aggregate within a spherical envelope of diameter d_e . The envelope diameter d_e is related to the aerodynamic diameter of the particle by the relation

$$\frac{d_e}{d_a} = \Phi^{-1/2} \left(\frac{C_a}{C_e}\right)^{1/2} \left(\frac{\zeta}{\zeta_o}\right)^{1/2}$$
 (B-24)

where ζ is the bulk density of the particle in g/cm³, $\zeta_0 = 1$ g/cm³; φ is the packing density, which is the ratio of the space actually occupied by primary particles in the envelope to the overall envelope volume; and C_x is the slip factor given by the expression:

$$C_x = 1 + 2\frac{\lambda}{d_x} \left[1.257 + 0.4 \exp \left[-\left(\frac{0.55d_x}{\lambda} \right) \right] \right]$$
 (B-25)

in which $\lambda \approx 8 \times 10^{-6} \text{cm}^3$ is the mean free path of air molecules at standard conditions. In the diesel particle model of Yu and Xu (1986), ζ has a value of 1.5 g/cm³ and a φ value of 0.3 is chosen based upon the best experimental estimates. As a result, Equation B-24 gives $d_e/d_a = 1.35$.

In determining the deposition fraction of DEPs, d_e is used for diffusion and interception according to the particle model.

B.5.1. Determination of $(DF)_H$

Particle deposition in the naso- or oropharyngeal region is referred to as head or extrathoracic deposition. The amount of particles that enters the lung depends upon the breathing mode. Normally, more particles are collected via the nasal route than by the oral route because of the nasal hairs and the more complex air passages of the nose. Since the residence time of diesel particles in the head region during inhalation is very small (about 0.1 s for human adults at normal breathing), diffusional deposition is insignificant and the major deposition mechanism is impaction. The following empirical formulas derived by Yu et al. (1981) for human adults are adopted for deposition prediction of DEPs:

For mouth breathing:

$$(DF)_{H,in} = 0, \text{ for } d_a^2 \le 3000$$
 (B-26)

$$(DF)_{H, in} = -1.117 + 0.324 \log(d_a^2 Q), for d_a^2 Q > 3000$$
 (B-27)

$$(DF)_{H, ex} = 0, (B-28)$$

and for nose breathing:

$$(DF)_{H, in} = -0.014 + 0.023 \log(d_a^2 Q), \text{ for } d_a^2 Q \le 337$$
 (B-29)

$$(DF)_{H, in} = -0.959 + 0.397 \log(d_a^2 Q), for d_a^2 Q > 337$$
 (B-30)

$$(DF)_{H, ex} = 0.003 + 0.033 \log(d_a^2 Q), \text{ for } d_a^2 Q \le 215$$
 (B-31)

$$(DF)_{H, ex} = -0.851 + 0.399 \log(d_a^2 Q), for d_a^2 Q > 215$$
 (B-32)

where $(DF)_H$ is the deposition efficiency in the head, the subscripts in and ex denote inspiration and expiration, respectively, d_a is the particle aerodynamic diameter in μm , and Q is the air flowrate in cm³/sec.

Formulas to calculate deposition of diesel particles in the head region of children are derived from those for adults using the theory of similarity, which assumes that the air passage in the head region is geometrically similar for all ages and that the deposition process is

- 1 characterized by the Stokes number of the particle. Thus, the set of empirical equations from B-
- 2 26 through B-32 are transformed into the following form:
- 3 For mouth breathing:

$$(DF)_{H, in} = 0, for d_a^2 Q \le 3000$$
 (B-33)

$$(DF)_{H, in} = -1.117 + 0.972 \log K + 0.324 \log(d_a^2 Q), \text{ for } d_a^2 Q > 3000$$
 (B-34)

$$(DF)_{H = ex} = 0. ag{B-35}$$

4 and for nose breathing:

5 6

7

8

9

10

11

12

13

14

15

$$(DF)_{H, in} = -0.014 + 0.690 \log K + 0.023 \log(d_a^2 Q),$$

 $for \ d_a^2 Q \le 337$ (B-36)

$$(DF)_{H, in} = -0.959 + 1.191 \log K + 0.397 \log (d_a^2 Q), \text{ for } d_a^2 Q > 337$$
 (B-37)

$$(DF)_{H, ex} = 0.003 + 0.099 \log K + 0.033 \log(d_a^2 Q), \text{ for } d_a^2 Q \le 215$$
 (B-38)

$$(DF)_{H, ex} = 0.851 + 1.197 \log K + 0.399 \log(d_a^2 Q), \text{ for } d_a^2 Q > 215$$
 (B-39)

where K is the ratio of the linear dimension of the air passages in the head region of adults to that of children, which is assumed to be the same as the ratio of adult/child tracheal diameters.

For rats, the following empirical equations are used for deposition prediction of DEPs in the nose:

$$(DF)_{H, in} = (DF)_{H, ex} = 0.046 + 0.009 \log(d_a^2 Q), \text{ for } d_a^2 Q \le 13.33$$
 (B-40)

$$(DF)_{H, in} = (DF)_{H, ex} = -0.522 + 0.514 \log(d_a^2 Q), \text{ for } d_a^2 Q > 13.33$$
 (B-41)

B.5.2. Determination of $(DF)_T$ and $(DF)_A$

The deposition model adopted for DEPs is the one previously developed for monodisperse (Yu, 1978) and polydisperse spherical aerosols (Diu and Yu, 1983). In the model, the branching airways are viewed as a chamber model shaped like a trumpet (Figure B-2). The cross-sectional area of the chamber varies with airway depth, x, measured from the beginning of the trachea. At the last portion of the trumpet, additional cross-sectional area is present to account for the alveolar volume per unit length of the airways.

Figure B-2. Trumpet model of lung airways.

Inhaled diesel particles that escape capture in the head during inspiration will enter the trachea and subsequently the bronchial airways (compartment T) and alveolar spaces (compartment A).

Assuming that the airways expand and contract uniformly during breathing, the equation for the conservation of particles takes the form:

$$\beta(A_1 + A_2) \frac{\partial c}{\partial x} + Q \frac{\partial c}{\partial x} = -Qc\eta$$
 (B-42)

where c is the mean particle concentration at a given x and time t; A_1 and A_2 are, respectively, the summed cross-sectional area (or volume per unit length) of the airways and alveoli at rest; η is the particle uptake efficiency per unit length of the airway; β is an expansion factor, given by:

$$\beta = 1 + \frac{V_t}{V_l} \tag{B-43}$$

and Q is the air flow rate, varying with x and t according to the relation

$$\frac{Q}{Q_o} = 1 - \frac{V_x}{V_l} \tag{B-44}$$

where Q_0 is the air flow rate at x=0. In Equations B-43 and B-44, V_t is the volume of new air in the lungs and V_x and V_ℓ are, respectively, the accumulated airway volume from x=0 to x, and total airway volume at rest.

Equation B-42 is solved using the method of characteristics with appropriate initial and boundary conditions. The amount of particles deposited between location x_1 and x_2 from time t_1 to t_2 can then be found from the expression

$$DF = \int_{t_1}^{t_2} \int_{x_1}^{x_2} Qc \eta dx dt$$
 (B-45)

For diesel particles, η is the sum of those due to the individual deposition mechanisms described above, i.e.,

$$\eta = \eta_I + \eta_S + \eta_P + \eta_D \tag{B-46}$$

where η_I , η_S , η_P , and η_D are, respectively, the deposition efficiencies per unit length of the airway due to impaction, sedimentation, interception, and diffusion. On the basis of the particle model described above, the expressions for η_I , η_S , η_P , and η_D are obtained in the following form:

$$\eta_I = \frac{0.768}{L} (St)\theta. \tag{B-47}$$

21
$$\eta_S = \frac{2}{\pi L} [2\epsilon \sqrt{1 - \epsilon^{(2/3)}} - \epsilon^{1/3} \sqrt{1 - \epsilon^{2/3}} + \sin^{-1} \epsilon^{1/3}]$$
 (B-48)

$$\eta_P = \frac{4}{3\pi L} (\Gamma - \frac{\Gamma^3}{32}) \tag{B-49}$$

1

3 4

5

6 7

8 9

10

11

$$\eta_D = \frac{1}{L} [1 - 0.819 \exp(-14.63\Delta) - 0.0976 \exp(-89.22\Delta) - 0.0325 \exp(-228\Delta) - 0.0509 \exp(-125\Delta^{2/3})]$$
(B-50)

2 sfor Reynolds numbers of the flow smaller than 2000, and

$$\eta_D = \frac{4}{L} \Delta^{1/2} \ (1 - 0.444 \Delta^{1/2}) \tag{B-51}$$

for Reynolds numbers greater than or equal to 2000, where $ST=d_a^2u/(18\mu R)$ is the particle Stokes number, $\theta=L/(8R)$, $\epsilon=3\mu u_sL/(32uR)$, $\Gamma=d_e/R$, and $\Delta=DL/(4R^2u)$. In the above definitions u is the air velocity in the airway; μ is the air viscosity; L and R are, respectively, the length and radius of the airway; $u_s=C_ad_a^2/(18\mu)$ is the particle settling velocity; and $D=C_ekT(3\pi\mu d_e)$ is the diffusion coefficient with k denoting the Boltzmann constant and T the absolute temperature. In the deposition model, it is also assumed that η_I and $\eta_P=0$ for expiration, while η_D and η_S have the same expressions for both inspiration and expiration.

During the pause, only diffusion and sedimentation are present. The combined deposition efficiency in the airway, E, is equal to:

$$E = 1 - (1 - E_S) (1 - E_D)$$
 (B-52)

where E_D and E_S are, respectively, the deposition efficiencies due to the individual mechanisms of diffusion and sedimentation over the pause period. The expression for E_D and E_S are given by

$$1 - \sum_{i=1}^{3} \frac{4}{\alpha_{i}} \exp(-\alpha_{i}^{2} \tau_{D}) (1 - \sum_{i=1}^{3} \frac{4}{\alpha_{i}^{2}}) \exp \left[-\frac{4\tau_{D}^{1/2}}{\pi^{1/2} (1 - \sum_{i=1}^{3} \frac{3}{\alpha_{i}^{2}})} \right]$$
(B-53)

where $\tau_D = D\tau/R^2$ in which τ is the pause time and α_1 , α_2 , and α_3 are the first three roots of the equation:

$$J_o(\alpha) = 0 \quad . \tag{B-54}$$

in which J_o is the Bessel function of the zeroth order, and:

$$E_S = 1.1094\tau_S - 0.1604\tau_S^2, for \ 0 < \tau_S \le 1.$$
 (B-55)

17 and

$$E_S = 1 - 0.0069\tau_S^{-1} - 0.0859\tau_S^{-2} - 0.0582\tau_S^{-3},$$

 $for \ \tau_S > 1,$ (B-56)

where $\tau_s = u_s \tau / 2R$.

The values of (DF)_T and (DF)_A over a breathing cycle are calculated by superimposing DF for inspiration, deposition efficiency E during pause, and DF for expiration in the tracheobronchial airways and alveolar space. It is assumed that the breathing cycle consists of a constant flow inspiration, a pause, and a constant flow expiration, each with a respective duration fraction of 0.435, 0.05, and 0.515 of a breathing period.

7 8

9

10

11

12

13

14

1

2

3

4

5

6

B.5.3. Lung Models

Lung architecture affects particle deposition in several ways: the linear dimension of the airway is related to the distance the particle travels before it contacts the airway surface; the air flow velocity by which the particles are transported is determined by the cross-section of the airway for a given volumetric flowrate; and flow characteristics in the airways are influenced by the airway diameter and branching patterns. Thus, theoretical prediction of particle deposition depends, to a large extent, on the lung model chosen.

15 16

17

18

19

20

21

22

B.5.3.1. Lung Model for Rats

Morphometric data on the lung airways of rats were reported by Schum and Yeh (1979). Table B-1 shows the lung model data for Long Evans rats with a total lung capacity of 13.784 cm³. Application of this model to Fischer rats is accomplished by assuming that the rat has the same lung structure regardless of its strain and that the total lung capacity is proportional to the body weight. In addition, it is also assumed that the lung volume at rest is about 40% of the total lung capacity and that any linear dimension of the lung is proportional to the cubic root of the lung volume.

23 24 25

26

27

28

29

30

31

32

B.5.3.2. Lung Model for Human Adults

The lung model of mature human adults used in the deposition calculation of DEPs is the symmetric lung model developed by Weibel (1963). In Weibel's model, the airways are assumed to be a dichotomous branching system with 24 generations. Beginning with the 18th generation, increasing numbers of alveoli are present on the wall of the airways, and the last three generations are completely aleveolated. Thus, the alveolar region in this model consists of all the airways in the last seven generations. Table B-2 presents the morphometric data of the airways of Weibel's model adjusted to a total lung volume of 3000 cm³.

Table B-1. Lung model for rats at total lung capacity

Generation number	Number of airways	Length (cm)	Diameter (cm)	Accumulative volume ^a (cm)
1	1	2.680	0.340	0.243
2	2	0.715	0.290	0.338
3	3	0.400	0.263	0.403
4	5	0.176	0.203	0.431
5	8	0.208	0.163	0.466
6	14	0.117	0.134	0.486
7	23	0.114	0.123	0.520
8	38	0.130	0.112	0.569
9	65	0.099	0.095	0.615
10	109	0.091	0.087	0.674
11	184	0.096	0.078	0.758
12	309	0.073	0.070	0.845
13	521	0.075	0.058	0.948
14	877	0.060	0.049	1.047
15	1,477	0.055	0.036	1.414
16 ^b	2,487	0.035	0.020	1.185
17	4,974	0.029	0.017	1.254
18	9,948	0.025	0.016	1.375
19	19,896	0.022	0.015	1.595
21	39,792	0.020	0.014	2.003
22	79,584	0.019	0.014	2.607
25	318,336	0.017	0.014	7.554
24	636,672	0.017	0.014	13.784

^aIncluding the attached alveoli volume (number of alveoli = 3×10^7 , alveolar diameter = 0.0086 cm). ^bTerminal bronchioles.

Table B-2. Lung model by Weibel (1963) adjusted to 3000 cm³ lung volume

Generation number	Number of airways	Length (cm)	Diameter (cm)	Accumulative volume ^a (cm)
0	1	10.260	1.539	19.06
2	2	4.070	1.043	25.63
2	4	1.624	0.710	28.63
3	8	0.650	0.479	29.50
4	16	1.086	0.385	31.69
5	32	0.915	0.299	33.75
6	64	0.769	0.239	35.94
7	128	0.650	0.197	38.38
8	256	0.547	0.159	41.13
9	512	0.462	0.132	44.38
10	1,024	0.393	0.111	48.25
11	2,048	0.333	0.093	53.00
12	4,096	0.282	0.081	59.13
13	8,192	0.231	0.070	66.25
14	16,384	0.197	0.063	77.13
15	32,768	0.171	0.056	90.69
16 ^b	65,536	0.141	0.051	109.25
17	131,072	0.121	0.046	139.31
18	262,144	0.100	0.043	190.60
19	524,283	0.085	0.040	288.16
20	1,048,579	0.071	0.038	512.94
21	2,097,152	0.060	0.037	925.04
22	4,194,304	0.050	0.035	1,694.16
23	8,388,608	0.043	0.035	3,000.00

^aIncluding the attached alveoli volume (number of alveoli = 3×10^3 , alveolar diameter = 0.0288 cm).

^bTerminal bronchioles.

B.5.3.3. Lung Model for Children

The lung model for children in the diesel study was developed by Yu and Xu (1987) on the basis of available morphometric measurements. The model assumes a lung structure with dichotomous branching of airways, and it matches Weibel's model for a subject when evaluated at the age of 25 years, the age at which the lung is considered to be mature. The number and size of airways as functions of age t (years) are determined by the following equations.

B.5.3.3.1. *Number of airways and alveoli.* The number of airways $N_i(t)$ at generation i for age t is given by

$$N_i(t) = 2^i,$$
 for $0 \le i \le 20$ (B-57)

$$\begin{cases}
N_{21}(t) = N_r(t), \\
N_{22}(t) = N_{23}(t) = 0.
\end{cases}
\text{ for } N_r(t) \le 2^{21}$$
(B-58)

$$N_{21}(t) = 2^{21},$$
 { $N_{22}(t) = N_r(t) - 2^{21},$ for $2^{21} < N_r(t) \le 2^{22}$ (B-59) $N_{23}(t) = 0,$

$$N_{21}(t) = 2^{21},$$

 $\{ N_{22}(t) = 2^{22}, for N_r(t) > 2^{21} + 2^{22},$ (B-60)
 $N_{23}(t) = N_r(t) - 2^{21} - 2^{22}$

 where $N_r(t)$ is the total number of airways in the last three airway generations. The empirical equation for N_r which best fits the available data is

$$N_r(t) = \begin{cases} 2.036 \times 10^7 (1 - 0.926e^{-0.15}t), & t \le 8 \\ 1.468 \times 10^7, & t > 8 \end{cases}$$
 (B-61)

Thus, $N_r(t)$ increases from approximately 1.5 million at birth to 15 million at 8 years of age and remains nearly constant thereafter. Equations B-58 to B-60 also imply that in the last three generations, the airways in the subsequent generation begin to appear only when those in the preceding generation have completed development.

The number of alveoli as a function of age can be represented by the following equation according to the observed data:

$$N_A(t) = 2.985 \times 10^8 (1 - 0.919e^{-0.45}t)$$
 (B-62)

 The number of alveoli distributed in the unciliated airways at the airway generation level is determined by assuming that alveolization of airways takes place sequentially in a proximal

direction. For each generation, alveolization is considered to be complete when the number of alveoli in that generation reaches the number determined by Weibel's model.

B.5.3.3.2. *Airway size*. Four sets of data are used to determine airway size during postnatal growth: (a) total lung volume as a function of age; (b) airway size as given by Weibel's model; (c) the growth pattern of the bronchial airways; and (d) variation in alveolar size with age. From these data, it is found that the lung volume, LV(t) at age t, normalized to Weibel's model at 4800 cm³ for an adult (25 years old), follows the equation

$$LV(t) = 0.959 \times 10^{5} (1 - 0.998e^{-0.002}t) (cm^{3}).$$
 (B-63)

The growth patterns of the bronchial airways are determined by the following equations

$$D_i(t) - D_{iw} = \alpha_i [H(t) - H(25)],$$
 (B-64)

$$L_i(t) - L_{iw} = \beta_i [H(t) - H(25)],$$
 (B-65)

- where $D_i(t)$ and $L_i(t)$ are, respectively, the airway diameter and length at generation i and age t,
- D_{iw} and L_{iw} the corresponding values for Weibel's model, α_i and β_i are coefficients given by

$$\alpha_i = 3.26 \times 10^{-2} \exp[-1.183 \ (i+1)^{0.5}]$$
 (B-66)

$$\beta_i = 1.05 \times 10^{-6} \text{ exp } [10.1] (i+1)^{-0.2}]$$
 (B-67)

and H(t) is the body height, which varies with age t in the form

$$H(t) = 1.82 \times 10^{2} (1 - 0.725e^{-0.14}t) \ (cm).$$
 (B-68)

For the growth patterns of the airways in the alveolar region, it is assumed that

$$\frac{D_i}{D_{iw}} = \frac{L_i}{L_{iw}} = \frac{D_a}{D_{aw}} = f(t), \quad \text{for } 17 \le i \le 23$$
(B-69)

where D_a is the diameter of an alveolus at age t, $D_{aw} = 0.0288$ cm is the alveolar diameter for adults in accordance with Weibel's model, and f(t) is a function determined from

$$f(t) = \sqrt{\frac{16}{\sum_{i=0}^{16} \frac{\pi}{4} D_i^2(t) L_i(t) N_i(t)}{\sum_{i=17}^{23} \frac{\pi}{4} D_{iw}^2 L_{iw} N_i(t) + \frac{5\pi}{36} D_{aw}^3 N_A(t)}}}$$
(B-70)

1 2

3

4

5

6 7

B.6. TRANSPORT RATES

The values of transport rates $\lambda_{XY}^{(i)}$ for rats have been derived from the experimental data of clearance for diesel soot (Chan et al., 1981; Strom et al., 1987, 1988) and for the particleassociated organics (Sun et al., 1984; Bond et al., 1986; Yu et al., 1991). These values are used in the present model of lung burden calculation and are listed below:

$$\lambda_{HG}^{(i)} = 1.73 \ (i = 1,2,3)$$
 (B-71)

$$\lambda_{HB}^{(1)} = \lambda_{TB}^{(1)} = \lambda_{LB}^{(1)} = \lambda_{AB}^{(i)} = 0.00018$$
 (B-72)

$$\lambda_{HB}^{(2)} = \lambda_{TB}^{(2)} = \lambda_{LB}^{(2)} = \lambda_{AB}^{(2)} = 0.0129$$
 (B-73)

$$\lambda_{HB}^{(3)} = \lambda_{TB}^{(3)} = \lambda_{LB}^{(3)} = \lambda_{AB}^{(3)} = 12.55$$
 (B-74)

$$\lambda_{TG}^{(i)} = 0.693 \qquad (i = 1, 2, 3)$$
 (B-75)

$$\lambda_{AL}^{(1)} = 0.00068 \left[1 - \exp(-0.046m_A^{1.62}) \right]$$
 (B-76)

$$\lambda_{AL}^{(i)} = \frac{1}{4} \lambda_{AB}^{(i)} \qquad (i = 2,3)$$
 (B-77)

$$\lambda_{AT}^{(i)} = 0.012 \exp(-0.11 m_A^{1.76}) + 0.00068 \exp(-0.046 m_A^{1.62}) \quad (i = 1,2,3)$$
(B-78)

$$\lambda_A^{(1)} = \lambda_{AL}^{(1)} + \lambda_{AT}^{(1)} + \lambda_{AB}^{(1)} = 0.012 \exp(-0.11m_A^{1.76}) + 0.00086$$
 (B-79)

$$\lambda_A^{(2)} = \lambda_{AL}^{(2)} + \lambda_{AT}^{(2)} + \lambda_{AB}^{(2)} = 0.012 \exp(-0.11 m_A^{1.76}) + 0.00068 \exp(-0.046 m_a^{1.62}) + 0.0161$$
(B-80)

$$\lambda_A^{(3)} = \lambda_{AL}^{(3)} + \lambda_{AT}^{(3)} + \lambda_{AB}^{(3)} = 0.012 \exp(-0.11 m_A^{1.76}) + 0.00068 \exp(-0.046 m_A^{1.62}) + 15.7$$
(B-81)

where $\lambda_{XY}^{(i)}$ is the unit of day⁻¹, and $m_A = m_A^{(1)}$ is the particle burden (in mg) in the alveolar compartment.

Experimental data on the deposition and clearance of DEPs in humans are not available. To estimate the lung burden of DEPs for human exposure, it is necessary to extrapolate the transport rates $\lambda_{XY}^{(i)}$ from rats to humans. For organics, we assume that the transport rates are the same for rats and humans. This assumption is based upon the observation of Schanker et al. (1986) that the lung clearance of inhaled lipophilic compounds appears to depend only on their

lipid/water partition coefficients and is independent of species. In contrast, the transport rates of diesel soot in humans should be different from those of rats, since the alveolar clearance rate, λ_A , of insoluble particles at low lung burdens for human adults is approximately seven times that of rats (Bailey et al., 1982), as previously discussed in Chapter 4.

No data are available on the change of the alveolar clearance rate of insoluble particles in humans due to excessive lung burdens. It is seen from Equation B-79 that $\lambda_A^{(I)}$ for rats can be written in the form

$$\lambda_A^{(1)} = a \exp(-bm_A^c) + d$$
 (B-82)

where a, b, c, and d are constants. The right-hand side of Equation B-82 consists of two terms, representing, respectively, macrophage-mediated mechanical clearance and clearance by dissolution. The first term depends upon the lung burden, whereas the second term does not. To extrapolate this relationship to humans, we assume that the dissolution clearance term is independent of species and that the mechanical clearance term for humans varies in the same proportion as in rats under the same unit surface particulate dose. This assumption results in the following expression for $\lambda_A^{(1)}$ in humans

$$\lambda_A^{(1)} = \frac{a}{P} \exp[-b(m_A/S)^c] + d$$
 (B-83)

where P is a constant derived from the human/rat ratio of the alveolar clearance rate at low lung burdens and S is the ratio of the pulmonary surface area between humans and rats. Equation B-83 implies that rats and humans have equivalent amounts of biological response in the lung to the same specific surface dose of inhaled DEPs.

From the data of Bailey et al. (1982), we obtain a value of $\lambda_A^{(1)} = 0.00169$ day⁻¹ for humans at low lung burdens. This leads to P = 14.4. Also, we find S = 148 from the data of the anatomical lung model of Schum and Yeh (1979) for rats and Weibel's model for human adults. For humans less than 25 years old, we assume the same value for P, but S is computed from the data of the lung model for young humans (Yu and Xu 1987). The value of S for different ages is shown in Table B-3.

Table B-3. Ratio of pulmonary surface areas between humans and rats as a function of human age

Age (year)	Surface area	
0	4.99	
1	17.3	
2	27.6	
3	36.7	
4	44.7	
5	51.9	
6	58.5	
7	64.6	
8	70.4	
9	76.0	
10	81.4	
11	86.6	
12	91.6	
13	96.4	
14	101	
15	106	
16	110	
27	115	
28	119	
19	123	
20	128	
21	132	
22	136	
23	140	
24	144	
25	148	

The equations for other transport rates that have a lung-burden-dependent component are extrapolated from rats to humans in a similar manner. The following lists the values of $\lambda_{XY}^{(i)}$ (in day⁻¹) for humans used in the present model calculation:

$$\lambda_{HG}^{(1)} = 1.73 \ (i = 1,2,3)$$
 (B-84)

$$\lambda_{HB}^{(1)} = \lambda_{TB}^{(1)} = \lambda_{LB}^{(1)} = \lambda_{AB}^{(1)} = 0.00018$$
 (B-85)

$$\lambda_{HB}^{(2)} = \lambda_{TB}^{(2)} = \lambda_{LB}^{(2)} = \lambda_{AB}^{(2)} = 0.0129$$
 (B-86)

$$\lambda_{HR}^{(3)} = \lambda_{TR}^{(3)} = \lambda_{LR}^{(3)} = \lambda_{AR}^{(3)} = 12.55$$
 (B-87)

$$\lambda_{TG}^{(i)} = 0.693 \qquad (i = 1,2,3)$$
 (B-88)

$$\lambda_{AL}^{(1)} = 0.00068 \{1 - 0.0694 \exp[-0.046(m_A/S)^{1.62}]\}$$
 (B-89)

$$\lambda_{AL}^{(i)} = \frac{1}{4} \lambda_{AB}^{(i)} \qquad (i = 2, 3)$$
 (B-90)

$$\lambda_{AT}^{(i)} = 0.0694 \ \{0.012 \ \exp[-0.11(m_A/S)^{1.76}] + 0.00068 \ \exp[-0.046(m_A/S)^{1.76}]\} \ (i = 1, 2, 3)$$
(B-91)

$$\lambda_A^{(1)} = \lambda_{AL}^{(1)} + \lambda_{AB}^{(1)} + \lambda_{AT}^{(1)} = 0.0694 \{0.012 \exp[-0.11(m_A/S)^{1.76}]\} + 0.00086$$
(B-92)

$$\lambda_A^{(2)} = \lambda_{AL}^{(2)} + \lambda_{AT}^{(2)} + \lambda_{AB}^{(2)} = 0.0694\{0.012 \exp[-0.11(m_A/A)^{1.76}] + 0.0068 \exp[-0.046(m_A/S)^{1.76}]\} + 0.016$$
(B-93)

(B-94)

B.7. RESULTS

B.7.1. Simulation of Rat Experiments

To test the accuracy of the model, simulation results are obtained on the retention of diesel soot in the rat lung and compared with the data of lung burden and lymph node burden obtained by Strom et al. (1988). A particle size of 0.19 μ m MMAD and a standard geometric deviation, σ_g , of 2.3 (as used in Strom's experiment) are used in the calculation.

The respiratory parameters for rats are based on their weight and calculated using the following correlations of minute volume, respiratory frequency, and growth curve data.

Minute volume =
$$0.9 \text{W (cm}^3/\text{min)}$$
 (B-95)

Respiratory frequency =
$$475W^{-0.3}$$
 (1/min) (B-96)

where W is the body weight (in grams) as determined from the equation

$$W = 5+537T/(100+T)$$
, for $T \ge 56$ days (B-97)

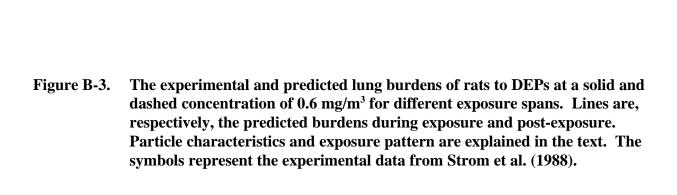
in which T is the age of the rat measured in days.

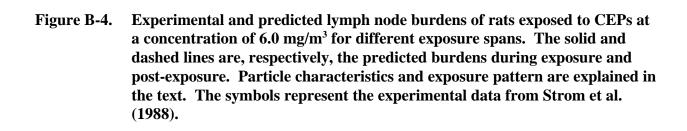
Equation B-95 was obtained from the data of Mauderly (1986) for rats ranging in age from 3 mo to 2 years old; Equation B-96 was obtained from the data of Strom et al. (1988); and Equation B-97 was determined from the best fit of the experimental deposition data. Figures B-3 and B-4 show the calculated lung burden of diesel soot ($m_A^{(I)} + m_T^{(I)}$) and lymph node burden, respectively, for the experiment by Strom et al. (1988) using animals exposed to DEPs at 6 mg/m³ for 1, 3, 6, and 12 weeks; exposure in all cases was 7 days/week and 20 h daily. The solid lines represent the calculated accumulation of particles during the continuous exposure phase and the dashed lines indicate calculated post-exposure retention. The agreement between the calculated and the experimental data for both lung and lymph node burdens during and after the exposure periods was very good.

Comparison of the model calculation and the retention data of particle-associated BaP in rats obtained by Sun et al. (1984) is shown in Figure B-5. The calculated retention is shown by the solid line. The experiment of Sun et al. consisted of a 30-min exposure to diesel particles coated with [${}^{3}H$] benzo[a]pyrene ([${}^{3}H$] - BaP) at a concentration of 4 to 6 µg/m 3 of air and followed by a post-exposure period of over 25 days. The fast and slow phase of ([${}^{3}H$] - BaP) clearance half-times were found to be 0.03 day and 18 days, respectively. These correspond to $\lambda_{AO}^{(2)} = 0.0385 \text{ day}^{-1}$ and $\lambda_{AO}^{(3)} = 23.1 \text{ day}^{-1}$ in our model, where $\lambda_{AO}^{(i)}$ is the value of $\lambda_{XY}^{(i)}$ at m_A \rightarrow 0. Figure B-5 shows that the calculated retention is in excellent agreement with the experimental data obtained by Sun et al. (1984).

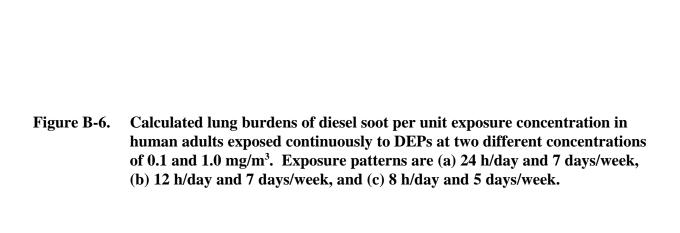
B.7.2. Predicted Burdens in Humans

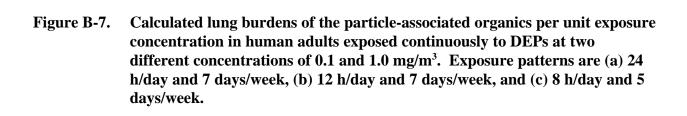
Selected results of lung burden predictions in humans are shown in Figures B-6 to B-9. The particle conditions used in the calculation are 0.2 μ m MMAD with $\sigma_g = 2.3$, and the mass fractions of the rapidly and slowly cleared organics are each 10% ($f_1 = f_2 = 0.1$). Figures B-6 and B-7 show, respectively, the lung burdens per unit concentration of diesel soot and the associated organics in human adults for different exposure patterns at two soot concentrations, 0.1 and 1 mg/m³. The exposure patterns used in the calculation are (a) 24 h/day and 7 days week; (b) 12 h/day and 7 days/week; and (c) 8 h/day and 5 days/week, simulating environmental and occupational exposure conditions. The results show that the lung burdens of both diesel soot and the associated organics reached a steady-state value during exposure. Because of differences in

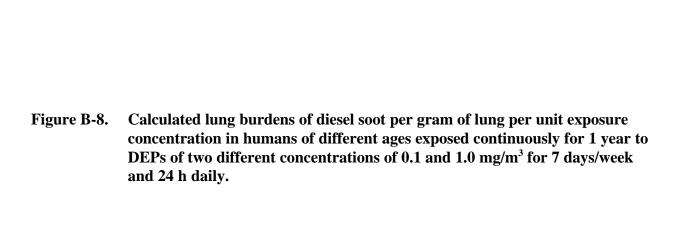


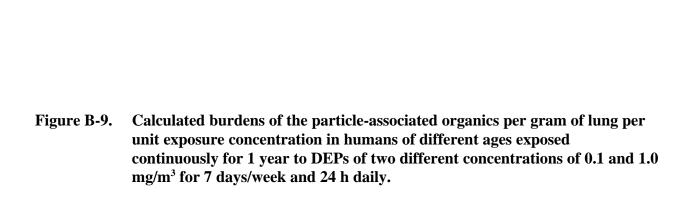












the amount of particle intake, the steady-state lung burdens per unit concentration were highest for exposure pattern (a) and lowest for exposure pattern (b). Also, increasing soot concentration from 0.1 to 1 mg/m³ increased the lung burden per unit concentration. However, the increase was not noticeable for exposure pattern (c). The dependence of lung burden on the soot concentration is caused by the reduction of the alveolar clearance rate at high lung burdens discussed above.

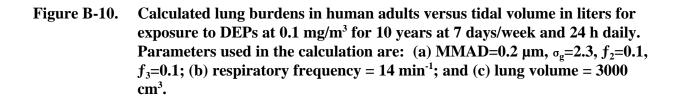
Figures B-8 and B-9 show the effect of age on lung burden, where the lung burdens per unit concentration per unit weight are plotted versus age. The data of lung weight at different ages are those reported by Snyder (1975). The exposure pattern used in the calculation is 24 h/day and 7 days/week for a period of 1 year at the two soot concentrations, 0.1 and 1 mg/m³. The results show that, on a unit lung weight basis, the lung burdens of both soot and organics are functions of age, and the maximum lung burdens occur at approximately 5 years of age. Again, for any given age, the lung burden per unit concentration is slightly higher at 1 mg/m³ than at 0.1 mg/m³.

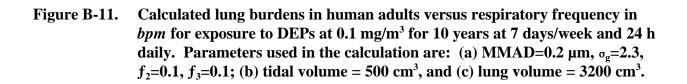
B.8. PARAMETRIC STUDY OF THE MODEL

The deposition and clearance model of DEPs in humans, presented above, consists of a large number of parameters that characterize the size and composition of diesel particles, the structure and dimension of the respiratory tract, the ventilation conditions of the subject, and the clearance half-times of the diesel soot and the particle-associated organics. Any single or combined changes of these parameters from their normal values in the model would result in a change in the predicted lung burden. A parametric study has been conducted to investigate the effects of each individual parameter on calculated lung burden in human adults. The exposure pattern chosen for this study is 24 h/day and 7 days/week for a period of 10 years at a constant soot concentration of 0.1 mg/m³. The following presents two important results from the parametric study.

B.8.1. Effect of Ventilation Conditions

The changes in lung burden due to variations in tidal volume and respiratory frequency are depicted in Figures B-10 and B-11. Increasing any one of these ventilation parameters increased the lung burden, but the increase was much smaller with respect to respiratory frequency than to tidal volume. This small increase in lung burden was a result of the decrease in deposition efficiency as respiratory frequency increased, despite a higher total amount of DEPs inhaled.

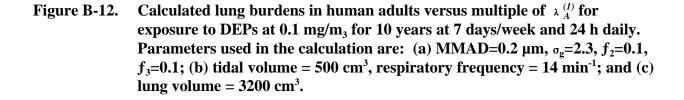


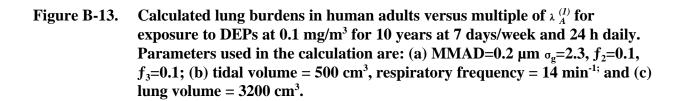


The mode of breathing has only a minor effect on lung burden because switching from nose breathing does not produce any appreciable change in the amount of particle intake into the lung (Yu and Xu, 1987). All lung burden results presented in this report are for nose breathing.

B.8.2. Effect of Transport Rates

Transport rates have an obvious effect on the retention of DEPs in the lung after deposition. Because we are mainly concerned with the long-term clearance of diesel soot and the associated organics, only the effects of two transport rates, $\lambda_A^{(I)}$ and $\lambda_A^{(2)}$, are studied. Experimental data of $\lambda_A^{(I)}$ from various diesel studies in rats have shown that $\lambda_A^{(I)}$ can vary by a factor of two or higher. We use a multiple of 0.5 to 2 for the uncertainty in $\lambda_A^{(I)}$ and $\lambda_A^{(2)}$ to examine the effect on lung burden. Figures B-12 and B-13 show respectively, the lung burden results for diesel soot and the associated organics versus the multiples of $\lambda_A^{(I)}$ and $\lambda_A^{(2)}$ used in the calculation. As expected, increasing the multiple of $\lambda_A^{(I)}$ reduced the lung burden of diesel soot with practically no change in the organics burden (Figure B-12), while just the opposite occurred when the multiple of $\lambda_A^{(I)}$ was increased (Figure B-13).





B.9. REFERENCES

Amann, CA; Siegla, DC. (1982) Diesel particles -- what are they and why. Aerosol Sci Technol 1:73-101.

Bailey, MR; Fry, FA; James, AC. (1982) The long-term clearance kinetics of insoluble particles from the human lung. Ann Occup Hyg 26:273-289.

Bond, JA; Sun, JD; Medinsky, MA; et al. (1986) Deposition, metabolism and excretion of 1-[¹⁴C]nitropyrene and 1-[¹⁴C]nitropyrene coated on diesel exhaust particles as influenced by exposure concentration. Toxicol Appl Pharmacol 85:102-117.

Chan, TL; Lee, PS; Hering, WE. (1981) Deposition and clearance of inhaled diesel exhaust particles in the respiratory tract of Fisher rats. J Appl Toxicol 1:77-82.

Diu, CK; Yu, CP. (1983) Respiratory tract deposition of polydisperse aerosols in humans. Am Ind Hyg Assoc J 44:62-65.

ICRP. (1979) Limits for intakes of radionuclides by workers. Ann ICRP 2. Publication 30, part 1.

Mauderly, JL. 1986. Respiration of F344 rats in nose-only inhalation exposure tubes. J Appl Toxicol 6:25-30.

Schanker, LS; Mitchell, EW; Brown, RA. (1986) Species comparison of drug absorption from the lung after aerosol inhalation or intratracheal injection. Drug Metab Dispos 14(1):79-88.

Scheutzle, D. (1983) Sampling of vehicle emissions for chemical analysis and biological testing. Environ Health Perspect 47:65-80.

Schum, M; Yeh, HC. (1979) Theoretical evaluation of aerosol deposition in anatomical models of mammalian lung airways. Bull Math Biol 42:1-15.

Snyder, WS. (1975) Report of task group on reference man. Oxford, London: Pergamon Press, pp. 151-173.

Solderholm, SC. (1981) Compartmental analysis of diesel particle kinetics in the respiratory system of exposed animals. Oral presentation at EPA Diesel Emissions Symposium, Raleigh, NC, October 5-7. In: Toxicological effects of emissions from diesel engines (Lewtas J, ed.). New York: Elsevier, pp. 143-159.

Strom, KA; Chan, TL; Johnson, JT. (1987) Pulmonary retention of inhaled submicron particles in rats: diesel exhaust exposures and lung retention model. Research Publication GMR-5718. Warren, MI: General Motors Research Laboratories.

Strom, KA; Chan, TL; Johnson, JT. (1988) Inhaled particles VI. Dodgson, J; McCallum, RI; Bailey, MR; et al., eds. London: Pergamon Press, pp. 645-658.

Sun, JD; Woff, RK; Kanapilly, GM; et al. (1984) Lung retention and metabolic fate of inhaled benzo(a)pyrene associated with diesel exhaust particles. Toxicol Appl Pharmacol 73:48-59.

Weibel, ER. (1963) Morphometry of the human lung. Berlin: Springer-Verlag.

Yu, CP. (1978) Exact analysis of aerosol deposition during steady breathing. Powder Technol 21:55-62.

Yu, CP.; Diu, CK; Soong, TT. (1981) Statistical analysis of aerosol deposition in nose and mouth. Am Ind Hyg Assoc J 42:726-733.

Yu, CP; Xu, GB. (1986) Predictive models for deposition of diesel exhaust participates in human and rat lungs. Aerosol Sci Technol 5:337-347.

Yu, CP; Xu, GB. (1987) Predicted deposition of diesel particles in young humans. J Aerosol Sci 18:419-429.

Yu, CP; Yoon, KJ, Chen, (1991) Retention modeling of diesel exhaust particles in rats and humans. Res Rep Health Eff Inst 40:1-24.